THE ASTROPHYSICAL JOURNAL, 397:L35–L38, 1992 September 20


# PRELIMINARY ANALYSIS OF AN ULTRAVIOLET *HUBBLE SPACE TELESCOPE* FAINT OBJECT CAMERA IMAGE OF THE CENTER OF M31[1]

I. R. KING,[2] J. M. DEHARVENG,[3] R. ALBRECHT,[4,5,6] C. BARBIERI,[7] J. C. BLADES,[8] A. BOKSENBERG,[9] P. CRANE,[5] M. J. DISNEY,[10] P. JAKOBSEN,[11] T. M. KAMPERMAN,[12] F. MACCHETTO,[6,8] C. D. MACKAY,[13] F. PARESCE,[6,8,14] G. WEIGELT,[15] D. BAXTER,[8] P. GREENFIELD,[8] R. JEDRZEJEWSKI,[8] A. NOTA,[8] W. B. SPARKS,[8] AND S. A. STANFORD[2]

*Received 1992 June 9; accepted 1992 July 9*

## ABSTRACT

A 5161 s exposure was taken with the FOC on the central 44″ of M31, through a filter centered at 1750 Å. Much of the light is redleak from visible wavelengths, but nearly half of it is genuine UV. The image shows the same central peak found earlier by Stratoscope, with a somewhat steeper dropoff outside that peak. More than 100 individual objects are seen, some pointlike and some slightly extended. We identify them as post–asymptotic giant branch stars, some of them surrounded by a contribution from their accompanying planetary nebulae. These objects contribute almost a fifth of the total UV light, but fall far short of accounting for all of it. We suggest that the remainder may result from the corresponding evolutionary tracks in a population more metal-rich than solar.

*Subject headings:* galaxies: individual: M31 — galaxies: nuclei — galaxies: stellar content

## 1. INTRODUCTION

Although elliptical galaxies and the central bulges of spirals are dominated by an old population showing a late-type spectrum, it has long been recognized (e.g., Code, Welch, & Page 1972) that many of them show an unexpected upturn in the ultraviolet, whose source has long been controversial. It has been attributed to a later forming stellar population, to post–asymptotic giant branch stars, to horizontal-branch stars, and to blue stragglers (Hills 1971; Tinsley 1971; Rose & Tinsley 1974; Ciardullo & Demarque 1978; Code & Welch 1979; Wu et al. 1980). *IUE* observations (Burstein et al. 1988 and references therein) and a rocket observation by Bohlin et al. (1985) have served to heat the controversy.

Neither stellar population models (full reference list in Greggio & Renzini 1990) based on the observed UV spectra nor the discovery of a correlation between the strength of the UV upturn and the galaxy metallicity (Faber 1983; Burstein et al. 1988) have allowed unambiguous conclusions as to the dominant contributor to the UV radiation.

The Faint Object Camera (FOC) team of the *Hubble Space Telescope* (*HST*) therefore decided to image the centers of the nearby galaxies M31 and M32, in an attempt (1) to map the distribution of the UV light; (2) to identify its sources, if possible; or (3) at the very least, to eliminate some of the possible candidates. M31 and M32 are of course particularly favorable for such a study, because of their small distance modulus.

## 2. OBSERVATIONS

M31 was observed on 1991 July 21 with the f/48 camera of the FOC, through filter F175W. (For details of the camera and its filters, see Paresce 1992). Exposures in fine lock were made in three successive *HST* orbits, with a total exposure time of 5161 s. The format was 512 × 1024 pixels, each of them zoomed to 50 × 25 μm giving a total field of 44″ × 44″. The images were flat-fielded and geometrically corrected by the Routine Science Data Processing "pipeline." The pipeline first divides each pixel into two equal ones, so as to change the image to a properly shaped 1024 × 1024. We removed the reseau marks ourselves, by interpolation, but left the blemishes.

For a general account of the performance of the FOC, see Greenfield et al. (1991).

The 512 × 1024 format has a counting capacity of only 255 per pixel, but none of our pixels exceeded this limit. This low count rate also kept our data in the linear domain of the detector. The dark count in the pixel-by-pixel sum of the three images, as estimated from the pixels within the shadow of the "slit finger," was 8 counts per pixel. At the time of these observations the f/48 detector was still not in perfect focus, so that the FWHM of point images is just under five 25 μm pixels, or about 200 mas.

Full analysis of the observations will take considerable time and effort, but we wish to make this preliminary report here. Figure 1 (Plate L8) reproduces the combined image.

[1] Based on observations with the NASA/ESA *Hubble Space Telescope*, obtained at the Space Telescope Science Institute, which is operated by AURA, Inc., under NASA contract NAS 5-26555.

[2] Astronomy Department, University of California, Berkeley, CA 94720.
[3] Laboratoire d'Astronomie Spatiale du CNRS, Traverse du Siphon, Les Trois Lucs, F-13012, Marseille, France.
[4] Space Telescope European Coordinating Facility.
[5] European Southern Observatory, Karl-Schwarzschild Strasse 2, D-8046 Garching, Germany.
[6] Affiliated to the Astrophysics Division, Space Science Department of ESA.
[7] Osservatorio Astronomico di Padova, Vicolo Osservatorio 5, I-35122 Padova, Italy.
[8] Space Telescope Science Institute, 3700 San Martin Drive, Baltimore, MD 21218.
[9] Royal Greenwich Observatory, Madingley Road, Cambridge CB3 0EZ, United Kingdom.
[10] Department of Physics, University College of Cardiff, P.O. Box 713, Cardiff CF1 3TH, Wales, United Kingdom.
[11] Astrophysics Division, Space Science Department of ESA, ESTEC, NL-2210 AG, The Netherlands.
[12] Laboratory for Space Research, Utrecht, Space Research Institute, Beneluxlaan 21, NL-3527 MS, The Netherlands.
[13] Institute of Astronomy, Cambridge, Madingley Road, CB3 0HA, United Kingdom.
[14] Osservatorio Astronomico di Torino.
[15] Max Planck Institut für Radioastronomie, Auf dem Hügel 69, D-5300 Bonn 1, Germany.

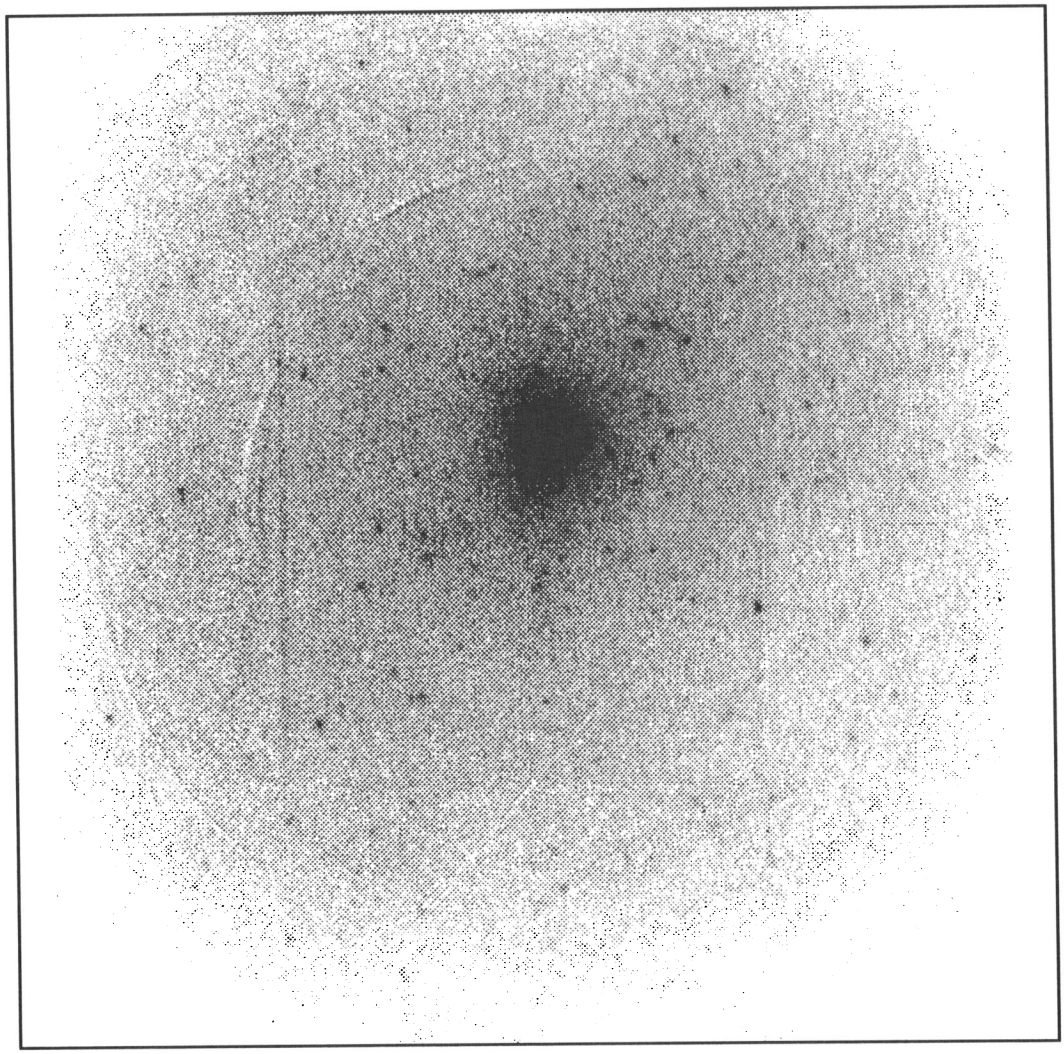

FIG. 1.—The composite 5161 s image of the center of M31, taken with the *HST* FOC f/48 camera and filter F175W. The image is 44″ on a side, and its vertical points toward P.A. 268°.

KING et al. (see 397, L35)

## 3. DISTRIBUTION OF LIGHT

Most of the light in our image has a smooth elliptical distribution. To derive the true profile we of course had to correct for the spherical aberration. For this we used a Fourier deconvolution, since the aesthetically more pleasing nonlinear methods do not preserve photometric values.

The PSF that we used is surely not perfect, since it was taken with a blue star, while the light coming through the large redleak of the filter has a PSF that is not exactly the same. We believe nevertheless that for an object with extended features such as M31 has, the deconvolution is quite satisfactory for the purpose of deriving a radial profile.

For analysis of the light distribution we used the PROFILE routine in the SunVista package. It fits elliptical isophotes to annuli 1 pixel wide, and gives the surface brightness on each of them. To achieve a wider spacing, we reran the routine on successively more compressed (and thus smaller) versions of the image, in order to get a smoother curve in the outer parts. The axial ratios were about 0.8, with the major axes in position angle about 70°. The assembled 45° axis profile is shown in Figure 2. Also shown there are the results of several sets of ground-based photometry data (including two unpublished ones by one of us [I. R. K.], which help connect the tiny Stratoscope [Light, Danielson, & Schwarzschild 1974] $V$-band domain with the wider one covered by other published studies). Within its limited accuracy, the profile of our deconvolved image resembles the ground-based profile, although the central peak found by Stratoscope is about twice as prominent in the UV.

Thus, even when we allow for a contribution from the filter redleak, it appears that the ultraviolet upturn comes from some component of the general population of the bulge, as was suggested by earlier UV observations (Deharveng et al. 1982; Welch 1982; Bohlin et al. 1985).

## 4. CALIBRATIONS

A photon at 175 nm has an energy of $1.13 \times 10^{-11}$ ergs; over the *HST* collecting area of $3.9 \times 10^4$ cm$^2$, a photon per second is equivalent to $2.9 \times 10^{-16}$ ergs cm$^{-2}$ s$^{-1}$. From the nominal prelaunch figures, a calculation of the integral of the product of the efficiencies of the telescope, the FOC, and the filter gives a result that is equivalent to a 100% transmission filter 4.8 Å wide. On-orbit calibration of the absolute sensitivity of the FOC (Sparks 1991) shows that the FOC sensitivity in this spectral region is 0.8 of nominal, so we reduce this figure to 3.8 Å. Thus a count per second corresponds, at 175 nm, to $F_\lambda = 7.6 \times 10^{-17}$ ergs cm$^{-2}$ s$^{-1}$ Å$^{-1}$. (A caveat attached to this calculation is that the absolute sensitivity measurements referred to have been made only in the f/96 camera, so we are assuming that the f/48 has suffered a similar decline.)

Not all the counts are due to UV photons, however. In addition to the small dark count, there is a serious problem of visible wavelength photons coming through the considerable redleak of the filter. This is a difficult quantity to determine. First, the redleaks of the FOC filters have not yet been measured on orbit, and we have to work with the nominal filter curves. Second, it is necessary to calculate the redleak contribution using a spectrum as similar as possible to that of M31. For this we used some models calculated some years before by Gustavo Bruzual to represent elliptical galaxies. These models had been made with a stellar mixture designed to reproduce the UV upturn observed in M31 and M32 by *IUE*.

We took the models that best fitted the observed $B-V$ color of M31 and calculated their expected counts through the F175W filter. The result, scaled to the observed $V$ magnitudes in M31, agreed with our observed level within a few tens of percent. Then on an $F_\lambda$ graph of the models multiplied by the sensitivity of the FOC used with the F175W filter, we estimated what fraction of the counts should be coming from below 2400 Å (a wavelength that in the graphs marked a minimum that seemed clearly to divide the redleak contribution from the in-band contribution) and what fraction from longer wavelengths. Our estimate is that the two numbers are approximately equal, so that about half of our counts come from true far-UV photons.

This is only a rough estimate, however. A figure that is probably more valid comes from a comparison with the flux

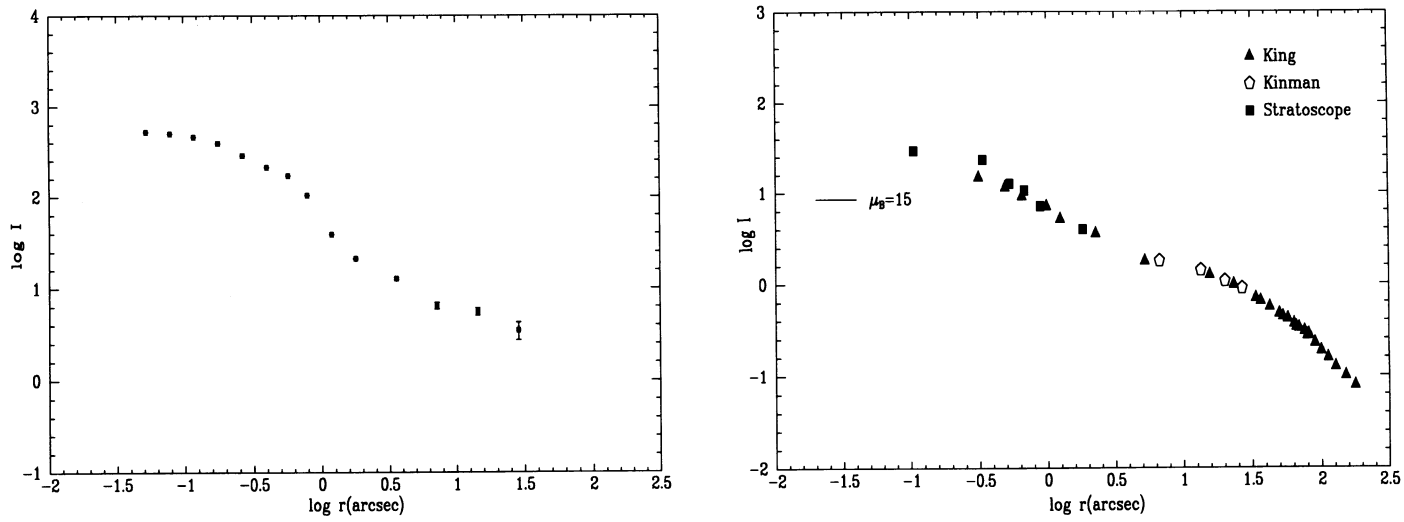


FIG. 2.—*Left*: Radial profile of the deconvolved *HST* image. *Right*: Ground-based profile of the same region. The sources, whose data have been fitted together with arbitrary shifts in log $I$, are from King (unpublished photographic photometry), Kinman (1965), and Light et al. (1974).

actually observed in this spectral region with *IUE*. The $F_\lambda$ observed by Burstein et al. (1988) is $7.45 \times 10^{-15}$ ergs cm$^{-2}$ s$^{-1}$ Å$^{-1}$ in this spectral region. In an area of 154 arcsec$^2$, centered on the central peak and equivalent to the effective area within their observing aperture, our total count rate was 256 s$^{-1}$, after correction for dark count. This would correspond to an $F_\lambda$ of $1.95 \times 10^{-14}$ if these were all true far-UV photons. Comparison with their $7.45 \times 10^{-15}$ would indicate then that 38% of our counts are true far-UV. Use of similar but independent figures from Welch (1982) confirms this figure closely. This is in reasonable agreement with the previous approximate evaluation of the redleak and is our best estimate until the observations taken for the calibration of the redleaks are fully reduced.

## 5. THE RESOLVED OBJECTS

Figure 1 shows a number of pointlike objects. We made a list of these by visual examination of the summed image and then verified their reality by blinking the three individual single-orbit images against each other and accepting only those that were clearly visible in the same location on at least two of the three images. Almost 150 objects survived.

Photometry of the objects is complicated by the gradient in the M31 background, especially near the center. To alleviate this problem, we fitted a smooth elliptic model to our radial profile and ellipticity of M31, and subtracted it from the image; this makes the objects much easier to measure, and any deviations of the subtracted profile from precise correctness are easily absorbed into the sky subtractions made for each star.

Our primary photometry was aperture photometry over a radius of 5 pixels, taking the sky value in an annulus between 10 and 15 pixels in radius. We shall refer to these magnitudes as APPHOT results.

In addition we made an independent set of magnitude measurements on Fourier deconvolutions of the images. Since the final stage of our deconvolution procedure endows each point image with a Gaussian profile, these images are well suited for the PSF-fitting procedure that DAOPHOT offers. We shall refer to these results as the NSTAR magnitudes.

As a check on the errors, which DAOPHOT estimates in only a formal way, we measured images 1 and 2 separately (APPHOT on the original image and NSTAR on the deconvolution) and compared the results between the two images in each case. We converted these single-image difference errors into the corresponding error in the sum of three images. The APPHOT measures turned out to be more accurate, and to reach fainter. The errors are a few hundredths of a magnitude for the brightest objects, but they increase to about half a magnitude at our limit of detection. They are not greatly in excess of the Poisson error associated with the image core that was used in the APPHOT measures. (There may be additional errors introduced by flat-fielding, however.)

A histogram of the APPHOT magnitudes is shown in Figure 3. The zero point conforms to the DAOPHOT convention that magnitude 25 corresponds to 1 count s$^{-1}$. The APPHOT magnitudes, however, refer to only the central core of the image and therefore need a correction for the missing outer light. We found from the growth curve of the PSF that a 5 pixel radius contains 0.114 of the light; thus the APPHOT zero point is too faint by 2.36 mag. There is also one more systematic correction to the APPHOT magnitudes; it arises from the fact that the sky measurement for each star, taken in the annulus from 10 to 15 pixels in radius around each star, includes some of the light

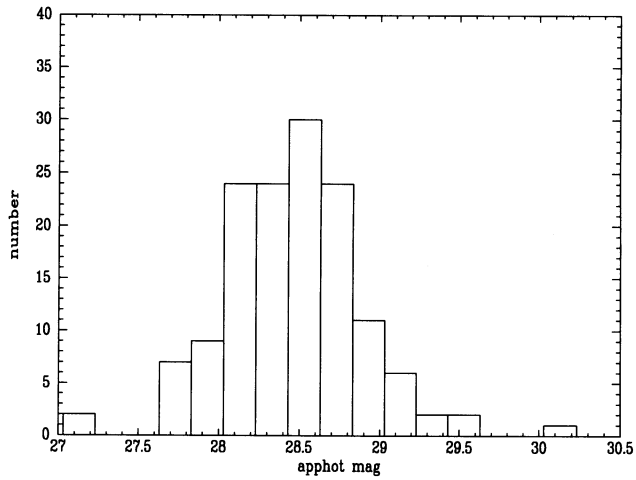


FIG. 3.—Numbers of objects in successive bins of apparent magnitude. The zero point is such that magnitude 27.60 corresponds to 1 detected count per second.

of the star. Following through the consequences of this effect shows (Holtzman & King 1992) that it affects each star by the same brightness factor; for the particular parameters of our measurements the dimming (from subtracting too high a sky value) is 0.24 mag. The total zero-point correction to the APPHOT magnitudes, to put them on a scale where magnitude 25 corresponds to 1 count s$^{-1}$ from the object, is thus 2.60 mag.

This zero-point correction is confirmed by the NSTAR magnitudes. Since the Fourier deconvolutions had used a normalized PSF, they had the effect of gathering all the original light of each star into its reconstructed image, and their NSTAR magnitudes therefore correspond to actual count per second values for each object. As a check on the APPHOT zero point, we took the difference between NSTAR and APPHOT magnitudes for the brightest 20 objects. The mean difference was 2.58 mag, in good agreement with the above result.

The APPHOT and NSTAR magnitudes show no systematic difference, other than the zero-point offset just discussed.

From the APPHOT magnitudes and the correction just derived, we find a total number of counts per second, from all the objects, of 6.41; with the zero-point correction of 2.60 mag this becomes 70.3 counts s$^{-1}$ in toto. The total counts s$^{-1}$ from the dark-subtracted image are 1456, so that the objects contribute 4.8% of the counts. But if we accept the redleak calculation that only 0.4 of the total counts are true UV, then the objects account for 12% of the UV flux.

The above figures do not take into account, however, the undoubted incompleteness of our faintest detections. To check on this we added to our images randomly placed objects having the same PSF, and repeated our finding operation. We did this at three different magnitudes, finding that we were 86% complete at APPHOT magnitude 28.5, 33% at 28.9, and 10% at 29.3. Thus the histogram in Figure 3 has incomplete numbers on the fainter side of its peak. In terms of total light, however, the corresponding correction is not great. We estimate that the 12% of the total UV flux calculated in the preceding paragraph will go up to 16% or 18% after incompleteness corrections are made more carefully.

We will give coordinates and magnitudes of the objects in a later paper. Their radial distribution does not appear to differ significantly from that of the M31 light.

## 6. INTERPRETATION

What are these objects? First, they must be very blue. For comparison with visible light we examined a 1 minute blue image taken with the Palomar 1.2 m Schmidt, which should show star images down to about $B = 19$. A central region slightly larger than our *HST* field was burned out, but the surroundings show no objects with any concentration toward the center of M31. Instead there is a thin, uniform distribution of stars, presumably belonging to the Galactic foreground. Counts of these stars indicate that approximately one of them should fall in our field, so our observed objects certainly belong to M31. Besides, they exhibit a gradual concentration to the center that is similar to that of the diffuse light. Calculations of stars of various spectral types as seen through the F175W filter show that the brighter of our objects would have a $B$ magnitude brighter than 19 if their spectral type were later than approximately B5.

A stronger test of the blueness comes from our UV image of M32 (not otherwise discussed here). For M32 we also have an exposure of 1500 s in the "$V$ band" (filter F480LP), which should reach to $V = 22$ or 23. The brightest UV object is totally invisible in our $V$ image, so it must be extremely blue.

Another clue is in the profiles of the objects. Of the brighter ones—where the profile has the greatest reliability—about half had a FWHM of 5 pixels, indistinguishable from the FWHM of PSFs observed in other images. But the other half had a FWHM averaging 7 pixels, indicating some extension.

It seems quite clear that our objects are post–asymptotic giant branch (PAGB) stars, around some of which planetary nebulae (PNs) can be seen. It should be noted that (1) PNs are much less conspicuous in the UV than their exciting stars (the emission lines adding up to only a few tens of angstroms of equivalent width of the stellar continuum), because the latter are hot objects that are so much brighter in the UV than the visible; (2) the stars with which we are dealing should be on a lower mass evolutionary track than those tracks that give rise to most of the PNs in the Milky Way around us, giving more time for the nebula to dissipate; and (3) as will be explained later, our wavelength band favors stars which are less hot, making it difficult to produce the stages of ionization from which the UV lines arise.

Detailed calculations are underway using published evolutionary tracks for PAGB stars (Schönberner 1981, 1983) and predictions of the number of such stars to be expected (Greggio and Renzini 1990). At this point we can say that the numbers and the fluxes that we observe are in order-of-magnitude agreement with these predictions, but definitive results will have to await a later publication.

As for the planetary nebula aspect of these objects, we made a comparison with the list given by Ciardullo et al. (1989), which includes and augments the previous list of Ford & Jacoby (1978). In both cases the PNs had been discovered by imaging in the 5007 Å line of [O III]. Nine of these PNs are in our field. By shifting the assumed center of M31 by an amount well within the positional uncertainty, we can match three of the PNs within 0".25. Of the others, two are obscured by reseau marks or cathode defects, two are too close to the edge of our image for clear identification, one is very faint in the Ciardullo et al. list, and only one is simply absent. Given that the far-UV lines and $\lambda$5007 are best excited by stars of different temperatures, we consider this imperfect agreement to be satisfactory. Note also that the far-UV PN lines come from ions of high ionization potential, and the hottest PAGB stars are lacking from our sample for photometric reasons: their flux is concentrated at wavelengths far shorter than our 1750 Å observing band.

As we saw above, the total contribution of the resolved objects identified as PAGB stars, corrected for incompleteness, is only 16%–18% of the total UV light. (This accords with the conclusion of Ferguson et al. 1991 that PAGB stars cannot account for the UV upturn in the light of the E galaxy NGC 1399, either.) It thus appears that the majority of the observed integrated UV flux comes from some component, too faint for us to resolve, that is distributed like the light in general.

A likely possibility could come from one factor that we have not considered up to this point: chemical abundance. Like the bulge of the Milky Way, the center of M31 must include a population whose heavy-element abundance considerably exceeds that of the Sun. That population would be expected to have evolutionary tracks quite different from those that are responsible for PAGB stars. Information regarding alternative late-evolution tracks is only now becoming available (Horch, Demarque, & Pinsonneault 1992; Castellani, Limongi, & Tornambé 1992), and our later paper will attempt to make predictions for them. Meanwhile we can only suggest that they might be the source of the missing UV flux.

I. R. King wishes to acknowledge his indebtedness to Jay Anderson for sensitivity calculations, and to Robin Clegg of Royal Greenwich Observatory for advice regarding planetary nebulae. The FOC IDT Support Team, D. Baxter, P. Greenfield, R. Jedrzejewski, and W. B. Sparks, acknowledge support from ESA through contract 6500/85/NL/SK. P. Crane and I. R. King acknowledge support from NASA through grants NAS5-27760 and NAG 5-1607.

## REFERENCES

Bohlin, R. C., Cornett, R. H., Hill, J. K., Hill, R. S., O'Connell, R. W., & Stecher, T. P. 1985, ApJ, 298, L37
Burstein, D., Bertola, F., Buson, L. M., Faber, S. M., & Lauer, T. R. 1988, ApJ, 328, 440
Castellani, M., Limongi, M., & Tornambè, A. 1992, ApJ, 389, 227
Ciardullo, R. B., & Demarque, P. D. 1978, in IAU Symp. 80, The HR Diagram, ed. A. G. D. Philip & D. S. Hayes (Dordrecht: Reidel), 345
Ciardullo, R., Jacoby, G. H., Ford, H. C., & Neill, J. D. 1989, ApJ, 339, 53
Code, A. D., & Welch, G. A. 1979, ApJ, 228, 95
Code, A. D., Welch, G. A., & Page, T. L. 1972, in The Scientific Results for the Orbiting Astronomical Observatory OAO-2 (NASA SP-310), 559
Deharveng, J. M., Joubert, M., Monnet, G., & Donas, J. 1982, A&A, 106, 16
Faber, S. M. 1983, Highlights Astron., 6, 165
Ferguson, H. C., et al. 1991, ApJ, 382, 69
Ford, H. C., & Jacoby, G. H. 1978, ApJ, 219, 437
Greenfield, P., et al. 1991, Proc. SPIE, 1494, 16
Greggio, L., & Renzini, A. 1990, ApJ, 364, 35
Hills, J. G. 1971, A&A, 12, 1
Holtzman, J. A., & King, I. R. 1992, in preparation
Horch, E., Demarque, P., & Pinsonneault, M. 1992, ApJ, 388, L53
Kinman, T. D. 1965, ApJ, 142, 1376
Light, E. S., Danielson, R. E., & Schwarzschild, M. 1974, ApJ, 194, 257
Paresce, F. 1992, Faint Object Camera Instrument Handbook, Version 3.0 (Baltimore: STScI)
Rose, W. K., & Tinsley, B. M. 1974, ApJ, 190, 243
Schönberner, D. 1981, A&A, 103, 119
———. 1983, ApJ, 272, 708
Sparks, W. B. 1991, Instrument Science Report FOC-053 (Baltimore: STScI)
Tinsley, B. M. 1971, A&A, 15, 403
Welch, G. A. 1982, ApJ, 259, 77
Wu, C.-C., Faber, S. M., Gallagher, J. S., Peck, M., & Tinsley, B. M. 1980, ApJ, 237, 290